

Faraday wave turbulence on a spherical liquid shell

R. Glynn 11011 and Eugene H. Trinh

(Jet Propulsion Laboratory, California Institute of Technology, Pasadena, CA 91109)

Abstract

Millimeter-radius liquid shells are acoustically levitated in an ultrasonic field. Capillary waves are observed on the shells. At low energies (minimal acoustic amplitude, thick shell) a resonance is observed between the symmetric and antisymmetric thin film oscillation modes. At high energies (high acoustic pressure, thin shell) the shell becomes fully covered with high-amplitude waves. Temporal spectra of scattered light from the shell in this regime exhibit a power-law decay indicative of turbulence. [PACS: 43.25.+y, 47.55.Dz, 47.35.+i, 47.27.-i]

draft, 6 May 96

Faraday wave turbulence on a spherical liquid shell

Introduction

Capillary waves are often observed on the surface of acoustically levitated drops, bubbles and shells [1]. The source of these capillary waves is a matter of some debate. Recent investigations [3] show that the onset of such waves in certain situations is threshold-dependent and occurs at (or near, see below) half the driving frequency. In these situations, the waves are not directly forced, rather they are parametrically excited by the forced low-amplitude oscillation of the interface in a direction normal to the surface at or near the acoustic field frequency. Thus, the fundamental energy-transfer mechanism is essentially the same as in the classical Faraday experiment [2], in which a container of liquid undergoes periodic translation oscillations along the gravity vector axis. The free surface of such a container of liquid is thus caused to vibrate periodically normal to its plane, and above a certain amplitude threshold capillary waves appear at half the driving frequency.

When we acoustically levitate a large shell (i.e. whose radius R is much larger than the capillary wavelength λ_c given by the dispersion relation

$$\omega^2 = \gamma k^3 / \rho \quad (1)$$

where ω is the frequency and k the wavenumber $2\pi / \lambda_c$, and γ and ρ are the fluid interfacial tension and density) capillary waves can appear in patches or on the whole surface of an otherwise quiescent shape. A unique feature of our system is that it is self-contained, boundary-free and contact-free: energy pumped into the system nonlocally by the acoustic field can be exchanged by nonlinear wave interactions on the shell, and can be damped by bulk viscosity and surface effects, but it is unaffected by contact with boundaries. There are no constraints on wave propagation on the shell except those self-selected by a resonance condition. The limiting wavenumber distribution reaches a steady-state characterized by the nonlinear wave interaction and the energy in the system.

In this Letter we wish to report some measurements we have made on the dynamics of large liquid shells. The liquid shells we observe in our lab are nearly spherical, have radii of the order of millimeters, and a fluid layer with thickness h of the order of tens to hundreds of microns. The shells are filled with and surrounded by air, and are positioned and manipulated by an external acoustic field as described below.

Description of the measurements and techniques

Figure 1 shows three successive images of an acoustically levitated shell in air. The acoustic field pressure amplitude P_a and frequency f_a are about 160 dB (re 20 μ Pa) and 20 kHz, respectively. The shell is formed from a solution containing pure water and a few drops of Kodak Photoflo™, a compound surfactant [4]. When measured via pendant drop tensiometry methods, the solution yields an equilibrium surface tension of 31 dyn/cm, with a surface relaxation time of the order of a second [5]. The bulk viscosity and density remain virtually unchanged from the values for pure water. An approximately 1 mm diameter droplet of solution is injected with air to form 3 to 8 mm diameter shells. Capillary waves arise on the shell as the shell evaporates and gets thinner in a constant acoustic pressure.

Spectral and amplitude information are obtained via laser scattering. For Fig. 2 and 3, an expanded, collimated, 3 mW He-Ne beam of 2 cm diameter is incident on the shell. A positive lens is placed roughly one focal length from the shell in the forward scattering direction along the optical axis. A stop is placed at the focal point behind the lens, blocking out the zeroth order Fourier component. A 6 mm diameter active area photodiode placed immediately after the stop gathers the light scattered into higher orders without discriminating between spatial frequency components. For Fig. 4, a 1 mW He-Ne beam is focussed onto a 90 micron diameter spot on the shell. The Doppler shift of the backscattered light from the surface of the shell is measured, and the resultant normal velocity component is obtained. The velocity information is then converted to a surface normal displacement amplitude. Spatiotemporal information is obtained from video with stroboscopic illumination and varying magnification factors.

Results and analysis

Figure 1 and Fig. 2 represent the events occurring in a typical shell lifetime. A typical experiment begins with the insertion of a thick shell into the acoustic field, where it is trapped at a pressure node of the acoustic standing wave. For 2-3 mm diameter shells, stable levitation is achieved at pressure levels below the onset of detectable capillary wave action [6], as shown in Fig. 1a. The shell appears to the naked eye (and to magnified video) as a nearly transparent, smooth surface, with pooling of excess liquid at the bottom of the shell due to gravity. The spatial FFT in Fig. 1a represents the non-oscillating background. The optical scattering spectrum (Figure 2, the spectra up to 100 seconds) has a dominant peak at **20.2** kHz, indicating that the shell interface is indeed moving periodically at the acoustic frequency at a low amplitude of about 500 nm peak. The other dominant peak in the low-amplitude/short-time regime is the fundamental shape mode frequency near 100 Hz.

As the shell thins, an abrupt transition occurs, as shown in Fig. 1b. Regular but dislocated patterns of waves with a single dominant wavelength (about 116 μm at 20 kHz) appear intermittently over the surface of the shell. Discrete peaks at $k_x = k_y = 0.054 \mu\text{m}^{-1}$ appear in the wavenumber space, reflecting the observation that a single wavenumber is being excited. However, two distinct peaks in the optical scattering spectrum appear (Fig. 2, the shaded peaks in the spectrum at 120 seconds through 270 seconds). The frequency separation between the peaks varies with shell thickness as much as a few hundred Hz. Nonlinear sum and difference peaks sometimes also appear.

Another abrupt transition from the dual-peaked behavior takes place as the shell thins below about 20 microns thickness (or if the pressure is increased substantially). Full isotropic coverage of the surface by a turbulent 'sea' of capillary waves is observed as shown in Fig. 1c. The spectrum of wavenumbers becomes broadband from $0.03 \leq |k| \leq 0.13 \mu\text{m}^{-1}$. The waves are so violent that, near the end of the shell's lifetime, microdroplets are ejected from the shell. This state is accompanied by the apparent elimination of gravity-induced pooling at the bottom, and an increased sphericity of the shell as a whole. The optical scattering spectrum becomes broadband in less than a second (Fig. 2, beginning at 2.80 seconds). Spectra taken during this

phase show two characteristic features: 1) a power-law decay of the spectrum from 2kHz to 20kHz; and 2) a persistence of a broad peak initially seen at 335 seconds, and marked by the 'x' at 1.5kHz at 375 seconds. This is accompanied by the apparent disappearance of the lower (squeezing mode of the film) peak.

Discussion

A. Dual peak spectra -- symmetric and antisymmetric wave resonance

A free liquid surface, when vibrated periodically and normal to its surface plane, will exhibit Faraday waves with *half* the driving frequency when the excitation overcomes the damping [2, 17]. Linear theory would predict a critical amplitude a_c of $2\nu k_0/\omega_a$, where ν is the bulk viscosity and k_0 is the onset wavenumber; For water, theory yields $a_c \approx 900$ nm, while a measurement just above the onset of measurable capillary wave action gives 1300 nm at the driving frequency, in fair agreement.

For a shell levitated in an acoustic standing wave in air there are two surfaces bounding the liquid. If $h \gg \lambda_c$, then (above the threshold forcing amplitude) pure capillary waves on both surfaces would be excited, with a frequency of $\omega_a/2$ and a wavelength given by (1). As $h \rightarrow \lambda_c$ the flow fields of each surface wave motion begin to interact, and energy must be divided between two possible modes of the shell wall -- symmetric (squeezing) and asymmetric (undulating) [7]. Assuming that the wavenumber remains constant (which measurements confirm), the frequencies for the new modes ω_+ (symmetric) and ω_- (antisymmetric) are no longer degenerate, and split about $\omega_a/2$. Above the threshold for Faraday waves, it can be shown that ω_+ and ω_- are nearly symmetric about $\omega_a/2$, and satisfy the resonance condition $\omega_a = \omega_+ + \omega_-$ postulated by Danilov and Mironov for a thin membrane in an acoustic field [8]. The capillary wave dispersion relation (1) now splits into:

$$\omega_+^2 = \frac{\gamma k^3}{\rho} \tanh\left(\frac{kh}{2}\right), \quad \omega_-^2 = \frac{\gamma k^3}{\rho} \coth\left(\frac{kh}{2}\right) \quad (2),$$

where at least initially the restoring force is still surface tension, and the waves are both capillary waves.

Figure 3 plots the normalized symmetric and antisymmetric wave mode frequencies as a function of the size parameter. When resonance obtains, kl is constant and equal to $k_0 = 0.054$ μm^{-1} , and the separation of the two peaks is a function of thickness. Our measurements agree with theory in the range $1 \leq kh \leq 2$, while the deviation at $kh = 0.5$ is probably due to the fact that our dispersion relations (2) are not valid in this thin regime.

B. Broadband spectra -- wave turbulence

Figure 4 shows the results of spectra taken from 17 different shells for fully developed, violent capillary waves covering the entire outer surface as in Fig 1c. Surface normal displacement power in nm^2 is plotted on a log scale in dB. The solid line is a best fit to all the spectra in the decay regime. A power-law is thus deduced for the power spectrum $S(\omega) \propto \omega^{-3.58 \pm 0.02}$, or very closely $\omega^{-18/5}$. The scaling exponent is insensitive to small variations in shell size, driving frequency, acoustic pressure, and material surface tension and surface viscosity.

The idea of wave interactions leading to weak and strong turbulence is not new [9]. What we believe is applicable to our situation is some form of resonant or near-resonant three-wave mixing: $k_1 + k_2 \approx k_3, \omega_1 + \omega_2 \approx \omega_3$ being simultaneously satisfied. Dispersion relations of the form (1) and (2) support such kinematic conditions [11]. Within this category there exist many theoretical predictions for power-law decay of wave spectra [9, 10].

Turbulence requires that inertial nonlinearities dominate linear damping in the temporal domain; *wave turbulence* further requires a broadband wavenumber spectrum, i.e. that nonlinear interactions dominate increased damping at higher wavenumbers than the onset wavenumber in the spatial domain. It is clear that the measurements reported here satisfy both requirements. It is much less certain how (or if) energy is distributed between the two available wave modes. To address this question we consider the damping of such modes.

Pure capillary waves satisfying (1) have a damping (at constant frequency) $\delta_c \propto \nu k^2$. The symmetric 'squeeze' mode damping is $\delta_s \propto h^3 k^4 / \nu$ [Vrij in 14]; the asymmetric 'bend' mode has a damping $\delta_b \propto \nu k^2$ [Joosten in 14]. 'J'bus, while the bend mode is clamped at essentially the same rate as pure capillary waves, the squeeze mode possesses a factor k^2 greater damping. At a

thickness of 2.0 microns, the damping ratio δ_4 / δ_0 is ~ 25 for the onset wavenumber $k_0 = 0.054 \mu\text{m}^{-1}$, and for $5k_0$ it is 625. Thus it is possible that we are observing only the bend mode in the turbulent regime.

We can constructively compare our results to those obtained with pure capillary waves on a plane surface in the standard Faraday experiment. Gollub and Ramshankar report a frequency decay exponent of 3.7 ± 0.2 for a vertically forced 8 cm square cell of n-butyl alcohol [12] driven with frequencies in the order of 100 Hz. Wright et al. [12] report a frequency decay exponent of 2.9 for a vertically forced 17 x 19 cm rectangular cell containing water and 1 μm polystyrene spheres. Since both authors use intensity fluctuations at a point to infer amplitude fluctuations in their frequency measurements, the difference could be due to the inherent nonlinearity of the scattered intensity. Wright et al. additionally report a directly measured wavenumber spectrum with a power-law decay of $k^{-4.6}$. Whether the difference between these and our results is a fluid effect, a boundary effect, dispersion-related or due to the method of measurement remains to be seen.

1) **Viscoelasticity and the dispersion relation**

in experimentation with other fluids, it becomes apparent that the surface viscoelasticity due to the added surfactant may be instrumental in allowing the shell to remain extant during the rather high-amplitude (typically 10 - 100 microns peak rms amplitude normal to the surface) wave motion in the turbulent regime. The inhibition of thinning well-known in soap films allows the study of our shells in 1 g, where drainage in water and low-viscosity silicone oil lead to breakup of the shell. This leads to the question of whether we might begin to see mixing of the capillary and elastic wave modes at these frequencies, which would cause a deviation of the effective dispersion away from the capillary relations (1) or (2) [15]. We have obtained sporadic capillary waves on shells of pure silicone oil (Trinh 1990 in [11, and present investigation), but we have as yet no quantitative data on pure liquids. The agreement of data with theory exhibited in Figure 3 indicates that elastic waves are not primarily observed in the dual-peaked regime. To

test for the presence of the elastic mode in the turbulent regime would require looking for a deviation of the ratio of the frequency spectrum to the wavenumber spectrum, since that ratio is determined by the dispersion relation. Wright et al. report that ratio to be within 20% of $d\omega/dk$ from (1) for their experiments with pure water.

In summary we have reported here the unique observations of wave resonance and turbulence in a contact-free continuous system. In contrast with hydrodynamic (vortex) turbulence, experiments exhibiting wave turbulence are very few [11,16]. To our knowledge, wave turbulence has never been observed or predicted for waves on a thin film. It is interesting that turbulence appears at all in such a relatively highly damped system. Many issues remain unexplored: primary among these is the nature of the dispersion relation in the turbulent regime [13], and in particular the effect of viscoelasticity introduced by surfactants.

“The research described in this paper was carried out at the Jet Propulsion Laboratory, California Institute of Technology, under contract with the National Aeronautics and Space Administration. We gratefully acknowledge the assistance of M. Barsoum in the acquisition of some of the spectra, A. Biswas for the laser vibrometer measurements, and thank J. Gollub for comments on an early version of this paper.

Footnotes

1. 1 {11. Trinh, in *Low Gravity Fluid Dynamics and Transport Phenomena*, J.N. Koster and R.L. Sani, eds., Progress in Astronautics and Aeronautics **130** (AIAA, Washington DC, 1990), p. 515; P.L. Marston *et al.*, in *Proceedings of the 'LA 1' Symposium on the First United States Microgravity Laboratory Mission, Huntsville, Alabama, 1993*, NASA CP-3272, Vol. 2, p. 673; E.G. Lierke *et al.*, in *Drops and Bubbles*, AIP Conference Proceedings No. 197, p. 71 (1988);
2. M. Faraday, Phil. Trans. Roy. Soc. 121, p 319 (1831); Benjamin, T.B. and F. Ursell, Proc. Roy. Soc. A 225, 505 (1954); Miles, J., J. Fluid Mech. **146, 285 (1984)**; J. Fluid Mech. 248, 671 (1993)
3. R.G. Holt and E.H. Trinh, APS Bulletin **39**, No. 9, DA6, p. 1887 (1994); R.G. Holt and D.F. Gaitan, APS Bulletin 40, No. 12, Dg8, p. 1960 (1995).
4. "There is some evidence for a steady (as opposed to a viscoelastic) stabilizing effect of compound surfactants on thin films or interfaces, see S. Singhal, C.C. Moser and M.A. Wheatley, Langmuir 9, 2426 (1993).
5. A.M. Worthington, Phil. Mag. **19**, 46 (1885); S.Y. Lin *et al.*, AIChE Journal 36, 1785 (1990); K. Stebe *et al.*, Phys. Fluids A **3**, 3 (1991).
6. Inelastic scattering techniques for capillary wave detection are much more sensitive than our Current method, and capable of detecting thermally driven fluctuations; they are not suitable for our present purposes. See D. Langevin, J. Chem. Soc. Faraday Trans. 1., 70, 95 (1974); R.B. Dorshow *et al.*, J. Appl. Phys. **63**, 1265 (1988); J. G. Joosten, J. Chem. Phys. **80**, 2383 (1984); D.S. Chung *et al.*, Phys. Lett. A **145**, 348 (1991); and R.C. Haskell *et al.*, Phys. Rev. E **47**, 439 (1993).
7. B.U. Felderhof, J. Chem. Phys. 49, 44 (1968).
8. S.D. Danilov and M.A. Mironov, J. Acoust. Soc. Am. 92, 2747 (1992).
9. For a broad review, see J.L. Hammack and D.M. Henderson, Annu. Rev. Fluid Mech. **25**, 55 (1993), and S.J. Putterman and P.H. Roberts, Phys. Rep, **168**, 209 (1988); also, V.F.

- Zakharov *et al.*, *Kolmogorov Spectra of Turbulence 1: Wave Turbulence*, Springer, Berlin, 1992); A.V. Kats and V.M. Kontorovich, *Z. Prikl. Mekh. Tekh. Fiz.*, No. 6, 97 (1974, translation by Khar'kov); A. Larraza *et al.*, *Phys. Rev. Lett.* **55**, 897 (1985); G. F. Falkovich *et al.*, *Europhys. Lett.* **29**, 1 (1995).
10. O.M. Phillips, *J. Fluid Mech.* **4**, 426 (1958) which he later disfavors: *J. Fluid Mech.* **156**, 505 (1985).
 11. A. Larraza and G. Falkovich, *Phys. Rev. B* **48**, 9855 (1993).
 12. J. P. Gollub and R. Ramshankar, in *New Perspectives in Turbulence*, 1.. Sirovich, ed. (Springer, New York, 1991), p. 165; W.B. Wright *et al.*, preprint.
 13. This may also involve a mode-dependent renormalization of the dispersion relation during the turbulent phase, see Larraza *et al.* in [9]. Additionally, if $kh \ll 1$ for the bend mode one can write $\omega^2 \sim 2\gamma k^2 / \rho h$. This would only accommodate *four*-wave mixing.
 14. Much work has been done on dispersion relations for viscoelastic surfaces and thin films: A. Vrij *et al.*, *Proc. K. Ned. Akad. Wet. Ser. B* **73**, 124 (1970); S. Sche and H.M. Fijnaut, *Surface Sci.* **76**, 186 (1978); J. G.H. Joosten, *J. Chem. Phys.* **80**, 2363 (1984); P. Sens *et al.*, *Langmuir* **9**, 3212 (1993); J. L. Harden and H. Pleiner, *Phys. Rev. E.* **49**, 1411 (1994); W. Cai and T.C. Lubensky, *Phys. Rev. Lett.* **73**, 1186 (1994).
 15. There is some evidence for capillary-to-elastic mode mixing: Y. Tian *et al.*, *Phys. Fluids* **7**, 2938 (1995); R.B. Dorshow and L.A. Turkevich, *Phys. Rev. Lett.* **70**, 2439 (1993); J.C. Fearnshaw *et al.*, *Phys. Rev. Lett.* **72**, 84 (1994).
 16. G.Z. Forristal, *J. Geophys. Res.* **86**, 8075 (1981); P. Hwang, (private communication); B. Jähne and K.S. Reimer, *J. Geophys. Res.* **95**, 11, S31 (1990).

Figure Captions

Figure 1: Series of three images of a 5mm diameter shell driven at 20.2 kHz and their spatial FFT's for a) a thick shell with no capillary waves; b) the onset of capillary wave action; and c) fully developed turbulent capillary waves. All three images share the same axes, and the units are mm. All three FFT's share the same axes, and the units are pm^{-1} . The scales for k_x and k_z differ by a factor of 4/3 due to the use of video imaging,

Figure 2: 27 measured spectra from the light-scattering experiment on a single shell as it evolves from thick to thin and bursts. The log of the power spectrum of scattered light into higher Fourier spatial orders was measured as a function of time ($f_{\text{Nyquist}} = 100 \text{ kHz}$). The data were segmented into 16 ms lengths, and a temporal FFT was performed. The horizontal axis in the plot is the frequency from 0 to 25 kHz. The logarithmic height axis is the spectral power. The depth axis is time. The displayed spectra are cinch RMS averages of 20 power spectra. The time between each displayed averaged spectrum is 20 seconds for the first 12, 10 seconds for the next 10, and 5 seconds for the last 6. The changing time scale is denoted by breaks in the axis.

Figure 3: The dispersion relation (2) for symmetric and antisymmetric waves versus the product of the wavenumber and the thickness. Theoretical results for ω_+ , ω_- , and their sum are plotted as continuous lines, the thick line is the sum $\omega_+ + \omega_-$. The dotted line at $\omega / \omega_a = 1$ indicates the resonance condition $\omega_a = \omega_+ + \omega_-$. Experimental observations for ω_+ (triangles), ω_- (upside-down triangles) and their sum (closed circles) are also plotted for $f_a = 20.2 \text{ kHz}$ and $k_o = 0.054 \mu\text{m}^{-1}$. The corresponding film thickness for fixed k_o is shown on the upper x axis.

Figure 4: The scaling range of measured spectra. The power spectrum $S(f)$ plotted is the average of 30 instantaneous spectra for displacement measured by integrating the velocity inferred from the Doppler-shifted backscattered light from a 90 micron beam spot of 1 $\mu\text{e-Ne}$ light incident on the shell surface. The displacement amplitudes were calibrated in nanometers, then the log of the power in nm^2 was converted to dB. The driving frequency is 22.189 kHz, and the shell diameter is 3.5 mm. The solid line is the best-fit power-law, with an exponent of 3.583-0.02.

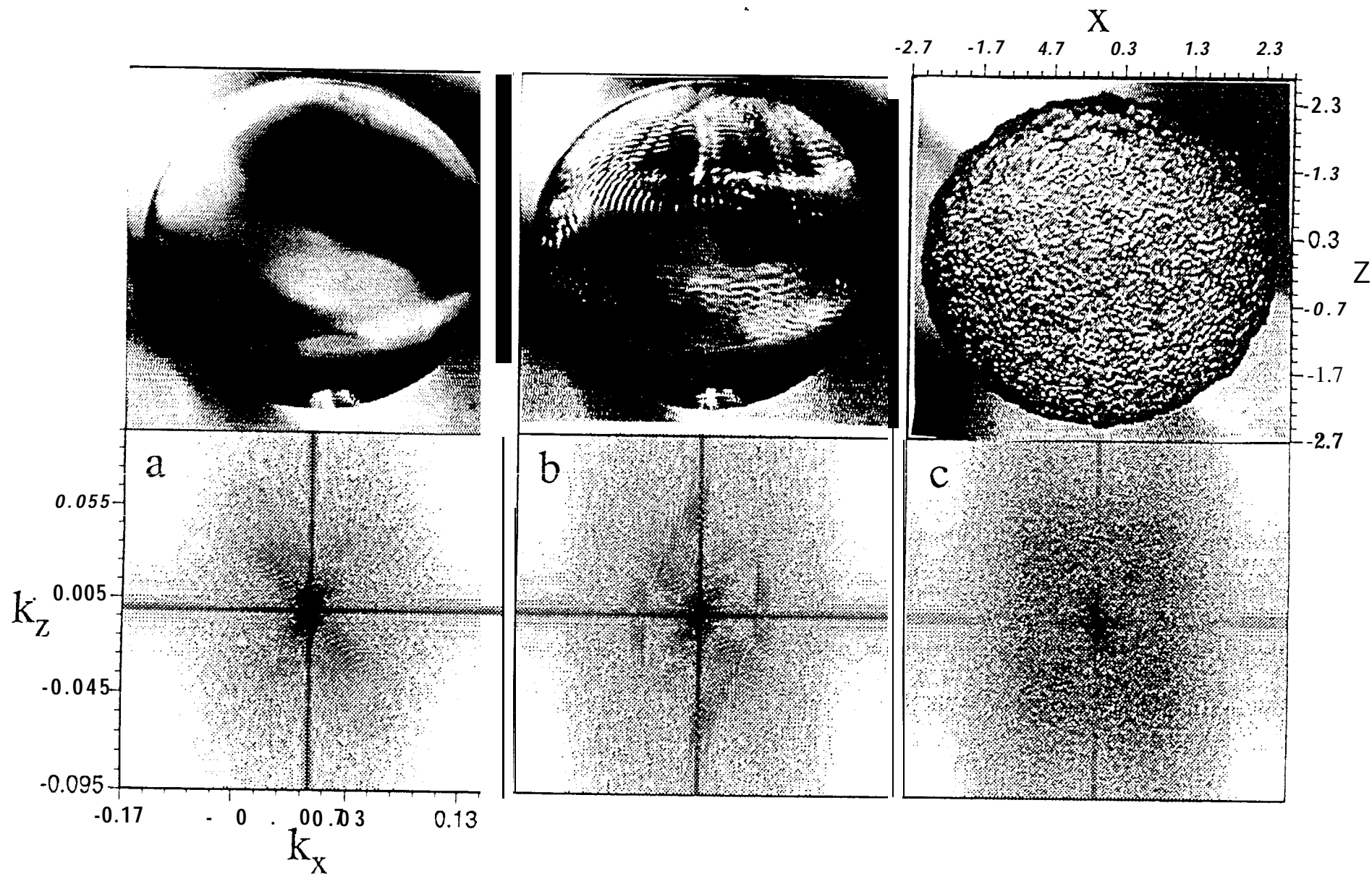


Fig 1

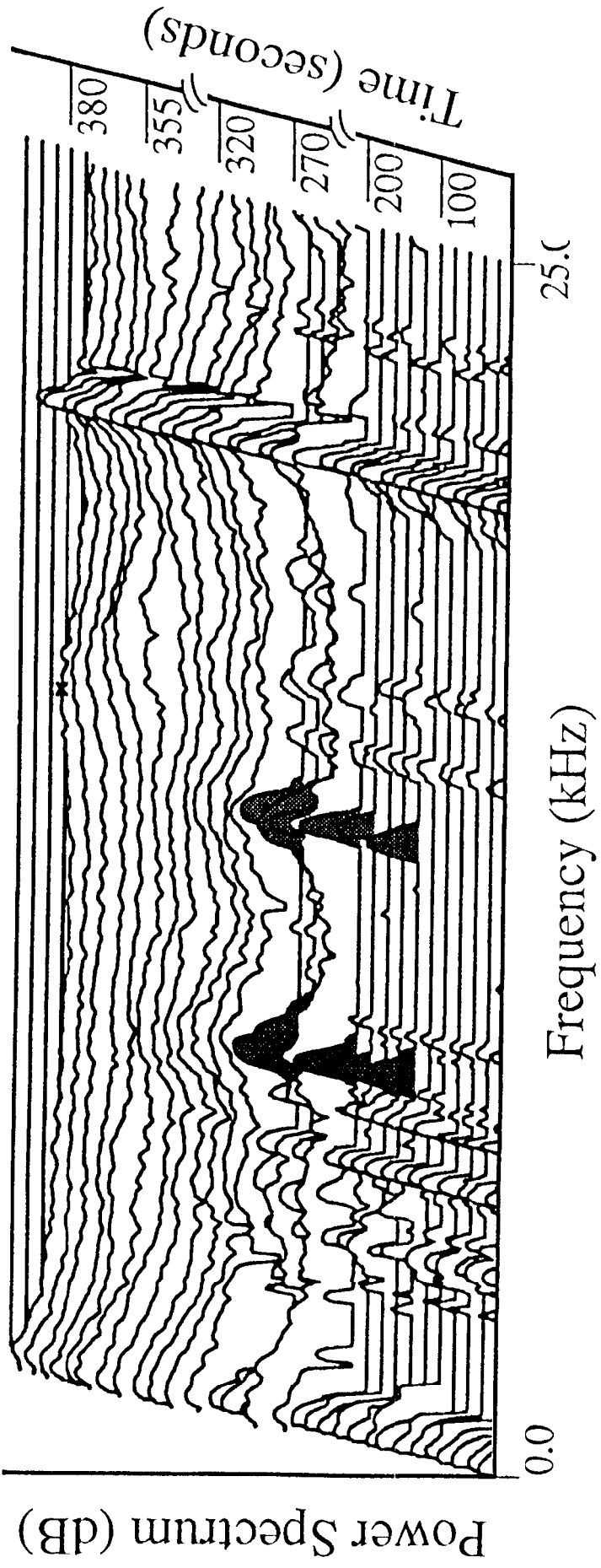


Fig 2

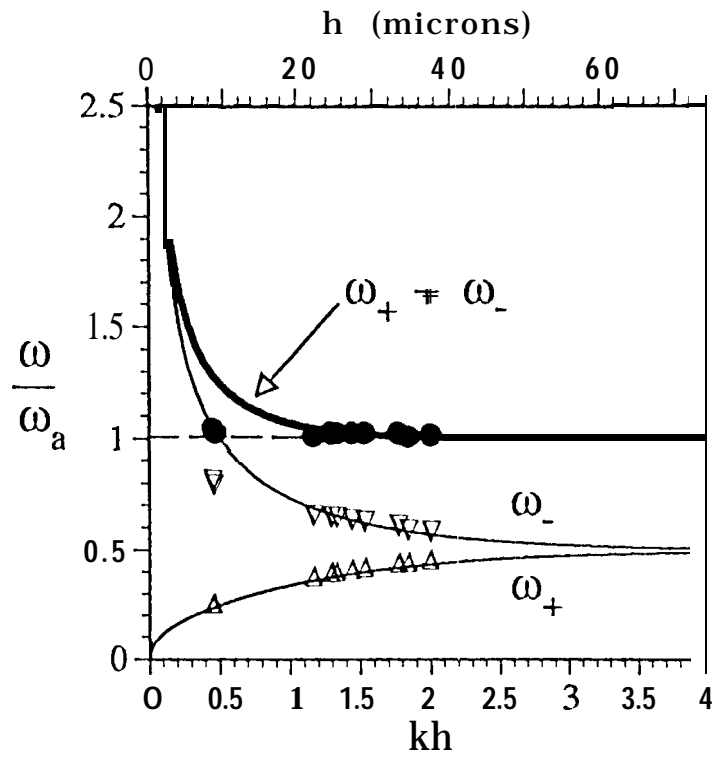


Fig 3

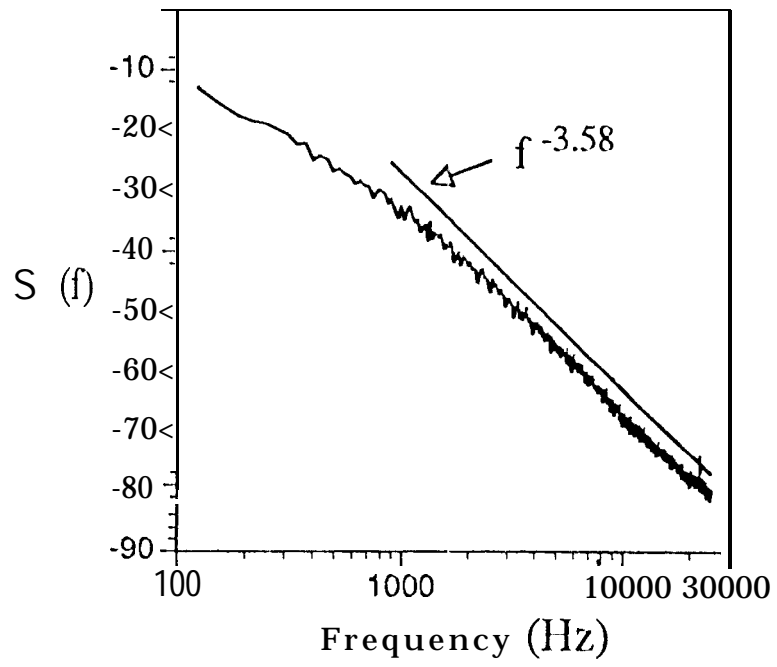


Fig 4